

EVOLUTION OF NUCLEAR STRUCTURE IN NEUTRON-DEFICIENT Pb ISOTOPES

J. PAKARINEN¹, R. WADSWORTH², A. ANDREYEV^{2,3}, S. EECKHAUDT¹,
T. GRAHN¹, P.T. GREENLEES¹, D.G. JENKINS², P. JONES¹, P. JOSHI², R. JULIN¹,
S. JUUTINEN¹, H. KETTUNEN¹, M. LEINO¹, A.-P. LEPPÄNEN¹, P. NIEMINEN¹,
R.D. PAGE³, J. PERKOWSKI¹, P. RADDON², P. RAHKILA¹, C. SCHOLEY¹,
J. UUSITALO¹, K. VAN DE VEL¹, D. WISEMAN³

¹*Department of Physics, University of Jyväskylä, P.O. Box 35,
FI-40014, Jyväskylä, Finland*

²*Department of Physics, University of York, Heslington,
York YO1 5DD, United Kingdom*

³*Department of Physics, Oliver Lodge Laboratory,
University of Liverpool, Liverpool L69 7ZE, United Kingdom*

1. Introduction

The atomic nucleus represents one of the fundamental building blocks of matter in the universe. In the heavy frontier, atomic systems that consist of nearly 300 nucleons have been synthesized. These complex systems give rise to a rich variety of quantum phenomena. As an exotic example, the interplay between single-particle motion, collectivity and pairing can result in nearly degenerate states of the same spin and parity in the same nucleus, but with different intrinsic structure. These states are often deformed and associated with different macroscopic shape. One of the richest regions exhibiting shape coexistence is formed by very neutron-deficient nuclei with the proton number Z close to the magic 82 and the neutron number N close to 104 midshell [1-3], where proton multiparticle-multihole structures intrude down to energies close to the spherical ground state. Producing Hard Copy Using MS-Word.

2. Development of shape coexistence theory in Pb region

The shape coexistence in this region was already discussed in 1960s by V.M. Strutinsky. He calculated energy differences between oblate and prolate nuclear equilibrium shapes using so-called shell correction method involving Nilsson orbitals [4]. Since then, this method has been called the Strutinsky shell-correction procedure and has proven to be a very useful tool for determining the ground state properties of atomic nuclei such as masses, deformations, etc. In paper by May, Pashkevich and Frauendorf, Strutinsky's shell correction method was applied for determination of deformation energies [5]. Using cranking model they found rotational energies for axially symmetric rotor. This allowed extracting oblate-prolate energy differences of low-lying yrast states.

A major step towards better understanding of coexisting structures in neutron deficient Pb isotopes was taken when Wood-Saxon average potential and monopole pairing interaction were applied to shell correction method. As a result, Bengtsson and Nazarewicz decomposed the ground state potential energy surface in separate parts characterized uniquely by the number of occupied intruder orbitals [6]. Their calculations produced the positions of the excited 0^+ intruder states. Intruders and proton multiquasiparticle structures were further discussed in Letter by Nazarewicz [7], in which he generated low-lying oblate and prolate shapes together with superdeformation.

The transition rates in neutron-deficient Pb nuclei were calculated, for the first time, by Bender and Heenan in 2004 [8]. They studied the low-lying collective excitations by performing a configuration mixing of angular momentum and particle-number projected self-consistent meanfield states employing Skyrme (Sly6) interaction. Their model qualitatively reproduced the variation of the spectra with neutron number and supported the picture of three different shapes lying close to the ground state.

The most recent theoretical efforts are made in the framework of interacting Boson model approximation (IBM). Hellemans et al. carried out detailed IBM calculations with configuration mixing and calculated energy levels and $B(E2)$ values for $^{188-196}\text{Pb}$ [9]. Furthermore, they extracted quadrupole deformations and the mixing between the different families in detail. Very recently, Nomura et al. found consistent evidence for shape coexistence in Pb region within the IBM plus configuration mixing with microscopic input based on the Gogny energy density functional [10].

3. Important experimental findings

Experimentally, shape coexistence in this region was first established in the early 1970's in laser spectroscopy experiments, in which a sudden change in nuclear charge radii was observed between ^{187}Hg and ^{185}Hg isotopes [11]. Since then a whole arsenal of experimental techniques have been developed to study this phenomenon. The low-lying 0^+ states were first identified in β -decay of mass separated Bi isotopes at Leuven ISOL facility [12]. α -decay fine structure measurements have probed the location of different minima, as a prime example a triplet of 0^+ states was found in ^{186}Pb [13,14]. Result from α - and β -decay experiment provided grounds for in-beam spectroscopic measurements, where rotational bands built on top of the deformed 0^+ states were investigated (see e.g. Ref. [15] and references therein). This includes both electron and γ -ray spectroscopy. Moreover, recent lifetime measurements employing Plunger-device have shed light on the collectivity of yrast transitions of neutron-deficient Pb isotopes [16].

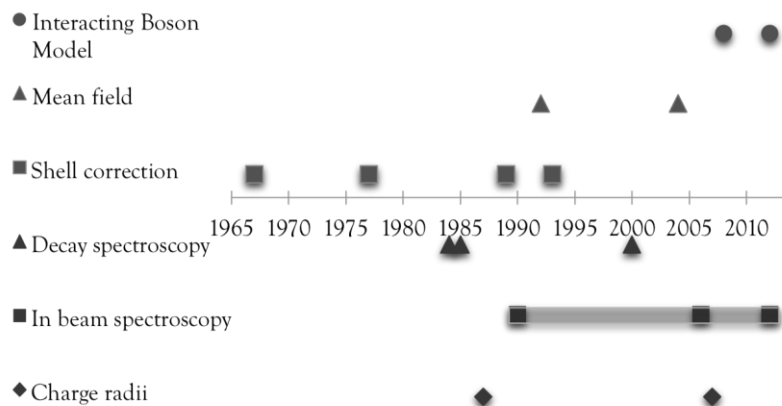


Figure 1. Some important theory and experiment milestones towards current understanding of shape coexistence in neutron-deficient Pb region. Different theoretical and experimental methods are shown in red and blue, respectively.

In addition, the shape of light even-mass Pb isotopes has been probed by measurement of optical isotope shifts providing mean square charge radii [17]. More evidence for shape coexistence in this region has also been gathered by investigating decay and band properties of isomeric states [18]. Interplay between theoretical and experimental research is illustrated on timeline in Fig.1. Taken the findings and substantial experimental and theoretical efforts put into investigation of shape coexistence phenomenon in Pb region, one could argue that it is well established. Nevertheless, there remain many intriguing questions: 1) *the role and behaviour of the multi-proton multi-hole excitations in odd-Z nuclei of $Z > 82$* , 2) *systematic behaviour of mixing between different shape coexisting structures*, 3) *explanation for identical structures observed in nuclei differing by an α -particle* and 4) *why is the collectivity of the prolate yrast bands in Pb nuclei higher than that of the identical prolate bands in Hg and Pt nuclei?*

Our experimental program employs in-beam spectroscopic methods in recoil-decay tagging experiments at the Accelerator Laboratory of Jyväskylä to address these matters. A prime example of power of that method is the in-beam γ -ray spectroscopy of ^{180}Pb , where proton-unbound states were observed. These nuclei can only be produced with cross section $\sim 10\text{nb}$ [19]. Structures of Pb isotopes beyond the $N=104$ midshell were further studied in in-beam γ -ray spectroscopy of odd-mass $^{183,85}\text{Pb}$ nuclei [20,21]. Results shed light on the coupling of an $i_{13/2}$ neutron hole to the yrast states of neighbouring even- A core. The recently developed SAGE spectrometer [22] was employed in simultaneous in-beam γ -ray conversion electron spectroscopy of ^{188}Pb [23]. Simultaneous γ -ray electron spectroscopy is needed to disentangle E0 strengths between states of the same spin and parity. In the following chapter, we report on the new results from in-beam γ -ray spectroscopy of ^{184}Pb .

4. In-beam γ -ray spectroscopy of ^{184}Pb – probing non-yrast states beyond the $N=104$ midshell.

The structures in beyond the neutron $N=104$ midshell nucleus ^{184}Pb were studied by employing the JUROGAM II+RITU+GREAT set-up. ^{184}Pb nuclei were produced via the $3n$ -fusion evaporation channel in the $^{83}\text{Kr}+^{104}\text{Pd}$ reaction at beam energy of 362MeV . The irradiation time was ~ 6 days and the production cross sections of ^{184}Pb was $\sim 3.5\mu\text{b}$. The beam intensity was limited

to $\sim 6\text{pnA}$ by the counting rates of the Ge-detectors at the target area, resulting in total counting rates of $\sim 250\text{Hz}$ at the focal-plane implantation detector.

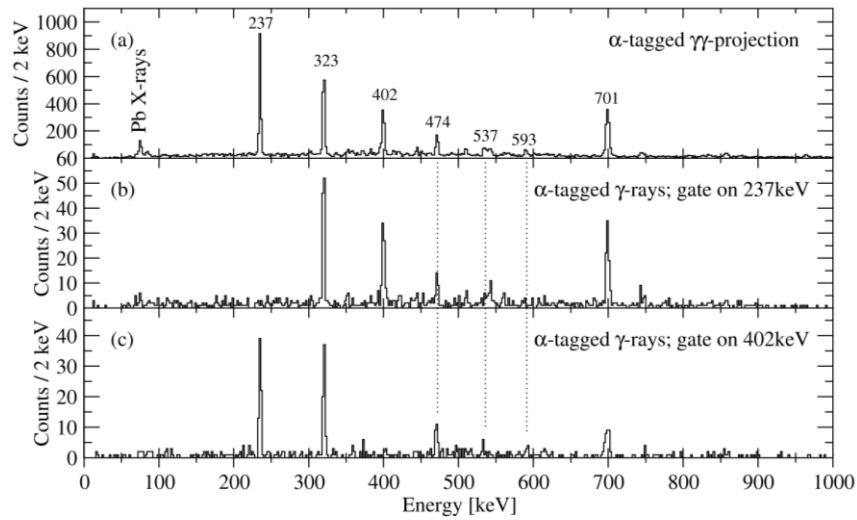


Figure. 2: The α -tagged $\gamma\gamma$ -coincidence spectra. The top spectrum shows mainly transitions belonging to the prolate yrast band. Gates on the $6^+ \rightarrow 4^+$ and $8^+ \rightarrow 6^+$ transitions are shown spectra b and c, respectively.

Prompt γ -rays were measured using the JUROGAM II Ge-detector array. Fusion evaporation residues were separated from the primary beam and transported to the focal plane using the gas-filled recoil-separator RITU [24], where they were implanted into the Double-Sided Silicon Strip Detector (DSSSD) of the GREAT spectrometer [25]. Detector signals were recorded using the triggerless Total Data Readout data acquisition system [26], where they were time stamped with a precision of 10ns. Prompt γ -rays detected in coincidence with implanted recoil and followed by a subsequent ^{184}Pb α -decay in the same DSSSD pixel within 900ms were selected in data analysis by employing the GRAIN analysis package [27]. In Fig. 2(a), recoil-gated, α -tagged singles γ -ray spectrum is shown. It mainly consists of typical sequence γ -rays associated with prolate yrast band in ^{184}Pb nucleus. An example of recoil-gated, α -tagged $\gamma\gamma$ -coincidence spectrum with gates on the 237keV and 402 keV transition are shown in Figs. 2(b) and 2(c), respectively. Based on similar conditions, three new transitions were found. The $\gamma\gamma$ -coincidence conditions allowed associating these transitions with the yrast cascade.

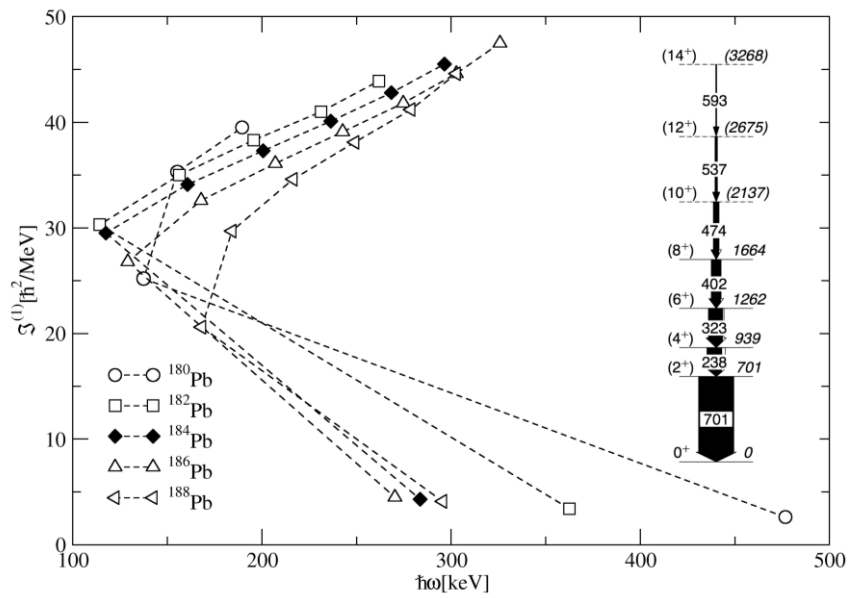


Figure. 3 Kinematic moment of inertia for yrast bands in neutron-deficient Pb isotopes. On right, partial level scheme for ^{184}Pb is shown.

According to γ -ray intensities and level energy systematics, these transitions are proposed to extend the known yrast band up to spin (14^+) . Partial level scheme is shown in the inset of Fig 3. All spin and parity assignments are tentative at the present stage of the analysis. The band shows similar behavior as the corresponding bands in neighboring even-mass ^{182}Pb and ^{186}Pb isotopes, which is illustrated in Fig. 3, where the kinematic moments of prolate bands in neutron-deficient Pb isotopes are plotted as a function of rotational frequency.

Summary

The studies of nuclear structure in Pb region have been very broad in scope. Versatile sets of tools, both theoretical and experimental, are required to advance our understanding of related phenomena. Very recently, post-accelerated radioactive beams in Pb region have become available allowing addressing remaining open questions from a new perspective.

References

1. J.L. Wood *et al.*, *Phys. Rep.* **215**, 101 (1992).
2. K. Heyde *et al.*, *Phys. Rev.* **C44**, 2216 (1991).
3. R. Julin *et al.*, *J. Phys.* **G27** R109 (2001).
4. V.M. Strutinsky, *Nuclear physics* **A95**,420 (1967).
5. F.R. May *et al.*, *Phys. Lett.* **B68**, 113 (1977).
6. R. Bengtsson and W. Nazarewicz., *Z. Phys.* **A334**, 269 (1989).
7. W. Nazarewicz, *Phys. Lett.* **B305**, 195 (1993).
8. M. Bender *et al.*, *Phys. Rev.* **C69**, 064303 (2004).
9. V. Hellemans *et al.*, *Phys. Rev.* **C77**, 064324 (2008).
10. K. Nomura *et al.*, *Phys. Rev.* **C86**, 034322 (2012).
11. J. Bonn *et al.*, *Phys. Lett.* **B38**, 308 (1972).
12. P. Van Duppen *et al.*, *Phys. Rev. Lett.* **52**, 1974 (1984).
13. P. Van Duppen *et al.*, *Phys. Lett.* **B154**, 354 (1987).
14. A. Andreyev *et al.*, *Nature* **405**, 430 (2000).
15. J. Pakarinen *et al.*, *Phys. Rev.* **C75**, 014302 (2007).
16. T. Grahn *et al.*, *Phys. Rev. Lett.* **97**, 062501 (2006).
17. H. De Witte *et al.*, *Phys. Rev. Lett.* **98**, 112502 (2007).
18. G.D. Dracoulis *et al.*, *Phys. Rev.* **C69**, 054318 (2004).
19. P. Rahkila *et al.*, *Phys Rev.* **C82**, 011303(R) (2010).
20. J. Pakarinen *et al.*, to be published
21. J. Pakarinen *et al.*, *Phys. Rev.* **C80**, 031303(R) (2009).
22. P. Papadakis *et al.*, *AIP Conf. Proc.* **1090**, 14 (2009).
23. P. Papadakis *et al.*, to be published
24. M. Leino *et al.*, *Nucl. Instrum. Methods Phys. Res.* **B99**, 653 (1995).

25. R.D. Page *et al.*, *Nucl. Instrum. Methods Phys. Res.* **B204**, 634 (2003).
26. I.H. Lazarus *et al.*, *IEEE Trans. Nucl. Sci.* **48**, 567 (2001).
27. P. Rahkila, *Nucl. Instrum. Methods Phys. Res.* **A595**, 637 (2008).